WO_x/ZrO_2 Catalysts Prepared by Anionic Exchange: In Situ Raman Investigation from the Precursor Solutions to the Calcined Catalysts

S. Loridant,* C. Feche, N. Essayem, and F. Figueras

Institut de Recherches sur la Catalyse/CNRS, UPR 5401, 2 av. A. Einstein 69626 Villeurbanne, France

Received: December 3, 2004; In Final Form: January 19, 2005

W/ZrO_2 catalysts were prepared using anionic exchange of peroxotungstate species with hydroxyl groups of zirconium hydroxide at low pH. The solids were dried and calcined under air at 700 °C. Each step of this novel method of preparation was investigated by Raman spectroscopy. A reference sample was also prepared by incipient wetness impregnation of $ZrO_2{\cdot}n(H_2O)$ with an ammonium tungstate solution and characterized throughout its preparation process. Complementary data were collected from X-ray diffraction, chemical analysis, surface area measurements, and thermal analysis. The Raman spectra of the $H_2WO_4-H_2O_2$ precursor solutions evidenced the presence of $(W_2O_3(O_2)_4(H_2O)_2)^{2-}$ dimers. These low-nuclearity species were exchanged with zirconium hydroxide at low pH. The Raman spectra of the dried solids did not reveal peroxotungstate species but were typical of tetrahedral $(WO_4)^{2-}$ species. A slight agglomeration of W species was observed with an increase in the W content. However, for an equivalent W loading, a higher W dispersion was obtained by anionic exchange, compared to the impregnation method. Furthermore, a remarkable homogeneity of the exchanged samples was evidenced by the micro-Raman spectra. The in situ Raman spectra recorded during calcination characterized both crystalline phases and supported tungsten species. Significant modifications were observed during the calcination process. The exchanged and the impregnated samples, with the same W loading, evidenced a similar type of tungsten species with one W═O bond. However, their behavior during calcination up to 700 °C was different. This was attributed to different strengths of interaction with the support. Moreover, the spectra recorded after calcination on various points of the exchanged sample with a high W content revealed a better spatial homogeneity than the impregnated one.

Introduction

Among the strong solid acid catalysts such as sulfated zirconia and heteropolyacids, tungstated zirconia is considered a very promising catalyst because of its high thermal stability under both reducing and oxidizing atmospheres. Therefore, these compounds could provide a good alternative for many reactions. The method of preparation of tungstated zirconia determines the catalytic properties. Indeed, it was reported that a catalyst prepared by impregnation of ZrO_2 was almost inactive for the isomerization of light alkanes, whereas a catalyst prepared by the reaction of tungstate molecular species and zirconium hydroxide followed by calcination under air at 800−850 °C was very active.[1,2]

In this study, a novel method of preparation of W/ZrO_2 catalysts was investigated thoroughly by in situ Raman spectroscopy. This original method consists of an anionic exchange between $H_2WO_4-H_2O_2$ aqueous solutions and zirconium hydroxide.[3] Indeed, without hydrogen peroxide, W species with a low nuclearity only exist in basic media. In these conditions, only impregnation can be achieved, because interactions between W species and the zirconia support are weak. An efficient anionic exchange between W species and hydroxyl groups of $ZrO_2{\cdot}nH_2O$ (PZC = 9) is only possible at acidic pH where isopolytungstates are stable in aqueous solutions. Nevertheless, the addition of H_2O_2 stabilizes some peroxotungstate species with a low nuclearity. Such species can be used to achieve anionic exchanges at low pH and may lead to higher W dispersions.

The catalysts obtained by this method, only dried, are active for the oxidation of dibenzothiophene by hydrogen peroxide, among other reactions. This reaction can be performed with good oxygen selectivities, with H_2O_2 in 2-butanol as the solvent, or in decane with *tert*-butyl hydroperoxide as oxidation agents.[4] The calcined samples are active in acidic-type reactions such as n-C_6 isomerization and Decaline hydroconversion. Their catalytic performances depend closely on the catalyst preparation parameters such as the W loading and the calcination temperature.[5]

Raman spectroscopy is a powerful technique to follow the preparation of materials, because spectra of precursor solutions can be obtained easily without the use a particular cell. The laser can be directly focused into the liquid under a microscope or by using an immersion probe. Furthermore, the Raman response of water is relatively weak by comparison with the IR one, and therefore, Raman spectra of aqueous solutions directly evidence the characteristic bands of dissolved molecular species. In addition, Raman spectroscopy is very valuable for in situ measurements, especially at high temperatures. Indeed, using a green exciting line allows the acquisition of Raman spectra up to typically 800 °C, because blackbody emission is low in the spectral range containing Raman bands. It is even possible to obtain Raman spectra at higher temperatures using a blue-shifted exciting line. Therefore, thermal treatment of materials can be easily investigated. Moreover, Raman spec-

* E-mail: loridant@catalyse.cnrs.fr. Phone: 0(033)472445334. Fax: 0(033)472445399.

10.1021/jp044494o CCC: $30.25
Published on Web 02/26/2005

TABLE 1: W Amounts, Specific Surface Areas, Surface W Loadings, XRD Data, and TGA Exothermic Peaks of the Support, $ZW_{0.01}$, $ZW_{0.05}$, $ZW_{0.1}$, and $ZW_{0.25}$ after calcination at 600 and 700 °C

	after calcination at 600 °C				after calcination at 700 °C				
sample	W (wt %)	SSA (m^2/g)	W surface content (W/nm^2)	phases observed by XRD	W (wt %)	SSA (m^2/g)	W surface content (W/nm^2)	phases observed by XRD	TGA exothermic peaks (°C)
$ZrO_2 \cdot n(H_2O)$		40−70 [10]	0.0	*m*-ZrO_2		20−40 [10]	0	*m*-ZrO_2	431
$ZW_{0.01}$	3.0	142	0.7	*m*-ZrO_2	3.2	49	2.0	*m*-ZrO_2	480
$ZW_{0.05}$	7.4	127	1.9	*t*-ZrO_2	7.9	87	3.0	*t*-ZrO_2	no
$ZW_{0.1}$	19.4	137	4.6	*t*-ZrO_2	19.2	89	7.2	*t*-ZrO_2	no
$ZW_{0.25}$	19.6	121	5.3	*t*-ZrO_2	19.8	91	7.1	*t*-ZrO_2	710

troscopy is especially suitable for the characterization of supported metal oxides, because the relative response of the support is usually lower than by IR spectroscopy and the structure of the support species can be determined by achieving spectra on pure powders under hydrated or dehydrated conditions.[6,7] Furthermore, the structural homogeneity of samples can be examined under a microscope with a probe of typically 1 μm.

Several authors evidenced that the catalytic properties of W/ZrO_2 only depend on the W surface density (W/nm^2). For instance, when it is slightly higher (8−10 W/nm^2) than the theoretical monolayer capacity of ZrO_2 (7 W/nm^2), the activity for the isomerization of *o*-xylene reaches a maximum.[8−10] This surface density can be modified by varying the tungsten loading and the calcination temperature.[8−10] In this paper, the importance of the method of preparation is highlighted. Indeed, each step of the anionic exchange method has been followed by Raman spectroscopy. The influence of some parameters such as the H_2WO_4 concentration, the $H_2WO_4-H_2O_2$ ratio, and the temperature of calcination is discussed. A standard catalyst has also been prepared and characterized in situ to compare the structure of the novel exchanged catalysts after drying and calcination up to 700 °C with this reference.

Experimental Section

Synthesis. WO_x/ZrO_2 catalysts were prepared by anionic exchange between H_2WO_4 dissolved in an aqueous solution of hydrogen peroxide and zirconium hydroxide. Hydrated zirconium hydroxide was precipitated at pH = 9 from a 0.4 M solution of $ZrOCl_2 \cdot 8H_2O$ (100 mL) and an ammonia solution (28%). The resulting suspension was aged for 20 min, separated by centrifugation, and washed with deionized water until complete elimination of chloride anions in the filtrate. The white gel was then dried at 110 °C for 24 h and crushed in automatic equipment.

Various quantities of H_2WO_4 were dissolved in H_2O_2 (aq, 35 wt %). The W concentrations of these aqueous solutions were 0.01, 0.05, 0.1, and 0.25 M. The exchange was achieved by the addition of 10 g of zirconium hydroxide in 150 mL of the prepared solutions. The suspension was stirred continuously for 15 min. Then, the solid was filtered, dried at 80 °C for 24 h, and eventually calcined at various temperatures. In the following, the resulting solids will be labeled $ZW_{0.01}$, $ZW_{0.05}$, $ZW_{0.1}$, and $ZW_{0.25}$. Two H_2O_2 aqueous solutions of H_2WO_4 0.5 M were also prepared to compare their Raman spectra with those of some exchanged solutions. Finally, some solutions with H_2O_2/W ratios lower than 10 were prepared but precipitated after few hours.

A sample was also prepared by impregnation of 1 g of zirconium hydroxide with 0.29 mL of ammonium metatungstate solution (0.23 M) at pH = 9. The solid was then dried in an oven for 12 h and calcined up to 700 °C in air. It will be abbreviated ZW_{imp} in the paper.

Characterization. X-ray diffraction (XRD) diagrams were obtained with a Bruker D5005 diffractometer using a Ni-filtered Cu Kα radiation (λ = 1.5418 Å). The presence of some crystalline phases was identified with the help of the Powder Diffraction File−International Centre for Diffraction Data (PDF−ICDD). Chemical analyses were performed by inductively coupled plasma spectroscopy (ICP) after dissolution of the samples. Thermal analysis curves were achieved with a Setaram 92.12 apparatus up to 1000 °C. Brunauer−Emmett−Teller (BET) surface areas were measured with a homemade apparatus from the adsorption isotherms at liquid nitrogen temperature after sample desorption at 250 °C under vacuum.

Raman spectra were recorded on raw powders at room temperature with a Dilor XY spectrometer. The exciting line at 514.53 nm of an argon laser was focused using a long-distance 50× objective. The size of the laser spot with such an objective was typically 2 μm. The spectra of solutions were obtained by directly focusing the laser in their upper parts.

The laser power used for the liquids and the powders was 15 and 5 mW, respectively. In any case, it was low enough to avoid the laser-heating effect. The wavenumbers obtained from the spectra are accurate to within 3 cm^{-1}. Thermal treatments were investigated by micro-Raman spectroscopy using a TS1500 linkam cell. The spectra of solids were recorded during an increase in the temperature up to 700 °C with a heating rate of ca. 3°/min. All the spectra achieved with the same laser power were normalized by dividing the signal by the accumulation time. The homogeneity of samples has been examined under the microscope before and after calcination by randomly selecting various points.

Results and Discussion

Table 1 sums up the XRD data obtained on the pure support and some exchanged catalysts calcined at 600 and 700 °C under air. The pattern of $ZW_{0.01}$ evidenced only monoclinic zirconia. When the tungsten loading was increased and reached the zirconium hydroxide exchange capacity, the tetragonal zirconia phase was stabilized and no WO_3 crystallites were detected by XRD after calcination up to 700 °C.

Figure 1 presents the Raman spectra of the $H_2WO_4-H_2O_2$ aqueous solutions used for the anionic exchanges with zirconium hydroxide. The H_2WO_4 concentration was varied from 0.5 to 0.1 M and the H_2O_2/W ratio from 22.6 to 113 (spectra a to c). The spectra of two additional solutions were also achieved for comparison: the first one (spectrum d) was a pure H_2O_2 aqueous solution (35 wt %) and the second one a solution for which the H_2WO_4 concentration was 0.5 M and the H_2O_2/W ratio equal to 10 (spectrum e). Spectrum a evidenced some bands at 955, 874, 850, 616, 553, and 313 cm^{-1}. The main band at 874 cm^{-1} was also observed with the pure H_2O_2 solution (spectrum d). It corresponds to the O−O stretching mode of hydrogen peroxide.[12] The relative intensity of the other bands decreased with a decrease in the W concentration. When the H_2O_2/W ratio was

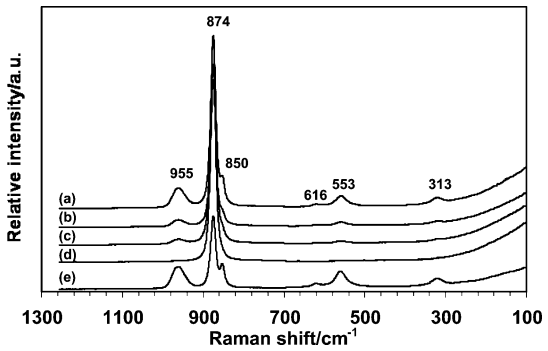

Figure 1. Raman spectra of H_2O_2 aqueous solutions of (a) H_2WO_4, 0.5 M with $H_2O_2/W = 22.6$; (b) H_2WO_4, 0.25 M with $H_2O_2/W = 45$; (c) H_2WO_4, 0.1 M with $H_2O_2/W = 113$; (d) H_2O_2 35 wt %; and (e) H_2WO_4, 0.5 M with $H_2O_2/W = 10$.

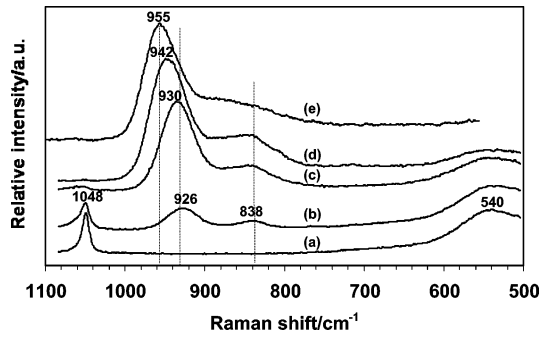

Figure 2. Raman spectra of dried samples: (a) support, (b) $ZW_{0.01}$, (c) $ZW_{0.05}$, (d) $ZW_{0.25}$, and (e) ZW_{imp}.

strongly decreased (spectrum e), they were always observed and their relative intensity was higher. Thus, these bands were assigned to some W species.

The Raman spectrum of large clusters such as the Dawson-type heteropolyanions $K_6P_2W_{18}O_{62}$ and the Keggin-type $H_3PW_{12}O_{40}$ evidenced strong W═O stretching bands at 992 cm^{-1} and other components at 920−960 cm^{-1} [13,14] and at 1014 and 988 cm^{-1},[15] respectively. The Raman spectra of various tungstate species present in aqueous solutions without H_2O_2 have been reported in the literature. When the pH is lowered, more aggregated species are observed. Then, the positions of $\nu_{W=O}$ stretching vibrations are shifted to higher frequencies in the same way as for heteropolytungstates. For instance, in tungstate aqueous solutions at pH = 5−7, the high-frequency bands were observed at 975−955 cm^{-1},[16−18] versus 990−975 cm^{-1} at pH = 2.[17]

The pH of the $H_2WO_4-H_2O_2$ solutions examined was less than 1. However, the highest-frequency Raman band was observed at 955 cm^{-1}. Therefore, polytungstate species were not present in these solutions. The observation of a narrow band at 850 cm^{-1} was an indication of the presence of a peroxo-tungstate species. The Raman bands of $(W_2O_3(O_2)_4(H_2O)_2)^{2-}$ in aqueous solution were observed at 960, 854, 622, 559, and 321 cm^{-1}.[12,15] It is likely that $(W_2O_3(O_2)_4(H_2O)_2)^{2-}$ was the main species in all the $H_2WO_4-H_2O_2$ solutions even for low H_2O_2/W ratios. The high-frequency bands could then be assigned to $\nu_{(W=O)}$, $\nu_{(O-O)}$, and $\nu_{s(W-O)}$, $\nu_{as(W-O)}$, and $\nu_{s(W-OH_2)}$ stretching modes, respectively.[12,15]

Figure 2 shows the Raman spectra achieved at room temperature of zirconium hydroxide and the exchanged solids after drying for 24 h at 80 °C. Several spectra were recorded under the microscope on various points of all these samples. They revealed a good spatial homogeneity with such a probe.

The support evidenced a narrow band at 1048 cm^{-1} attributed to the ν_1 vibrations of carbonate anions and a broad band around 540 cm^{-1} that could correspond to $\nu_{(Zr-OH)}$ vibrations. These bands disappeared with an increase in the W loading because of an anionic exchange. The bands characteristic of peroxo-tungstate species, and in particular, $(W_2O_3(O_2)_4(H_2O)_2)^{2-}$, were not observed anymore. It can be concluded that the peroxo-tungstate species were decomposed through an interaction with $ZrO_2 \cdot n(H_2O)$ and/or drying. However, the spectra of samples with a W content lower than 10 wt % (spectra b and c) presented two additional bands near 930 and 840 cm^{-1}, which could be attributed to the A_1 (ν_{sym}) and F_2 (ν_{asym}) vibration modes of $(WO_4)^{2-}$ anions in T_d symmetry.[13,19] Aqueous tungsten solutions at pH > 9 for which monomeric $(WO_4)^{2-}$ species are mainly present evidence very similar band positions.[16,17] However, the breadth of the A_1 band is then smaller and its relative intensity higher. When the symmetry of an MO_4 molecule is lowered, the triply degenerated F_2 mode is split, and additional bands are observed. The $(WO_4)^{2-}$ species evidenced in spectra b and c seem to have a T_d site symmetry. Accordingly, they could be located in the bulk after exchange with hydroxyl groups, forming an amorphous phase in which Zr^{4+} cations are surrounded by $(WO_4)^{2-}$. It was proposed previously that such an interaction would permit the crystallization of zirconia in the tetragonal phase during calcination.[20] Another possibility to obtain such a symmetry is that the interaction of W surface species with the support was weak and these species were surrounded by protons.

Very similar spectra were observed with various crystalline phases in which W cations are located in T_d sites. For instance, the Raman bands of the cubic Na_2WO_4 phase were observed at 929, 837, and 335 cm^{-1} [19] and correspond to internal vibrations of WO_4^{2-} tetrahedra with a bond length of ca. 1.82 Å.[21] In the tetragonal $SrWO_4$ structure, the W−O bond lengths are slightly longer (1.85 Å)[22] and the main ν_1 Raman band was evidenced at 921 cm^{-1}, [23] whereas in the monoclinic $ZnWO_4$ structure, these lengths are shorter (1.80 Å)[24] and the ν_1 band was observed at 955 cm^{-1}.[19] However, among tungstates of the scheelite type, there is no simple and general relationship between frequencies and interatomic distances.[25]

When the symmetry of W tetrahedra is lowered and some W−O bonds are shortened, the shape of spectra is completely changed, and the $\nu_{(W=O)}$ stretching bands are observed at much higher frequencies. For instance, in the cubic $Zr(WO_4)_2$ structure, WO_4 tetrahedra are located at C_3 sites. One of the four W−O bonds is significantly shorter (1.73 Å) than the three others (1.78 Å). The corresponding ν_1 vibrations were observed up to 1034 cm^{-1}.[26] In the same way, $(WO_4)^{2-}$ ions occupy two different sites with C_2 and C_1 symmetry in the orthorhombic $Al_2(WO_4)_3$ phase. The W−O bond lengths of the C_2 sites are 1.74 and 1.765 Å, and the corresponding ν_1 internal vibrations were observed around 1050 cm^{-1}. The W−O bond lengths of the C_1 sites are longer (1.76−1.78 Å), and the corresponding ν_1 Raman bands were located near 1000 cm^{-1}.[27]

At high W amount, the main band was shifted to 942 cm^{-1} and broadened (spectrum d). This shift is an indication of a symmetry lowering. It could also reveal a change of coordination and an aggregation of tungsten species. Finally, the main band of the impregnated sample was slightly narrower than that of $ZW_{0.25}$, and its maximum was observed at a higher wavenumber. Therefore, spectrum d could be considered a combination of spectra c and e.

Figure 2 underlines the influence of the method of preparation. Indeed, the main band of the impregnated sample was observed at a significantly higher frequency than $ZW_{0.25}$, which

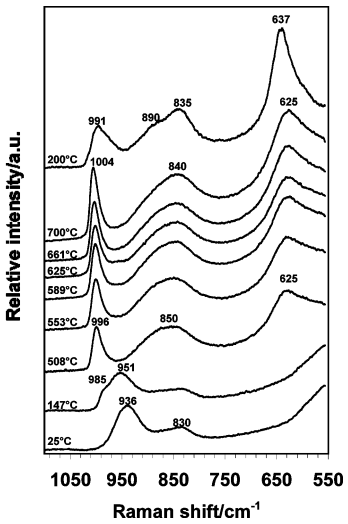

Figure 3. In situ Raman spectra recorded at various temperatures during calcination of $ZrW_{0.05}$ up to 700 °C.

has a close W content, suggesting a higher degree of agglomeration. The nature of the species in $ZW_{0.05}$ and ZW_{imp} was completely different: the first one contained mainly isolated WO_4 species, while in the second one, *para*-tungstate-type species could have been formed.[17] It was evidenced that the tetrahedral species have specific catalytic properties for dibenzothiophene oxidation, because the impregnated sample exhibits much lower activity than the exchanged ones.[4]

Figure 3 presents some Raman spectra recorded during the calcination of $ZW_{0.05}$ up to 700 °C. At 147 °C, the main band was shifted to 951 cm^{-1}, and a shoulder appeared at 985 cm^{-1}. From 200 up to 450 °C, a huge fluorescence was mainly observed and masked superimposed weak Raman bands. Above 500 °C, a narrow band was observed at 996 cm^{-1} and also two additional broad bands around 850 and 625 cm^{-1}. When the temperature reached 700 °C, the narrow peak was located at 1004 cm^{-1} and the two broad bands were located near 840 and 625 cm^{-1}. When the temperature was decreased to 200 °C under ambient air, the high-frequency band was downshifted to 991 cm^{-1} and significantly broadened. The widths of the other bands decreased, and their positions were measured at 637 and 835 cm^{-1}. An additional weak shoulder was also evidenced near 890 cm^{-1}.

The band at 637 cm^{-1} and some other broad bands observed at 455, 310, 270, and 150 cm^{-1} (not shown) are typical of nanocrystallites of tetragonal zirconia.[28] The Raman half-width at half maximum (HWHM) values of the bands at 270 and 150 cm^{-1} are 14 and 5.5 cm^{-1}, respectively, when the particle size is 7 nm.[28] It should be lower in the present study, because the corresponding HWHM values deduced from Raman spectra of $ZW_{0.05}$ at room temperature were around 40 and 20 cm^{-1}, respectively.

Tetragonal ZrO_2 is stabilized by a crystallite size effect according to the Gibbs−Thomson law.[29,30] For instance, when the crystallite size is lower than 7 nm, the tetragonal phase is stabilized at room temperature.[28] As already proposed,[31] tungsten oxide could inhibit the crystalline growth stabilizing nanocrystallites of metastable tetragonal ZrO_2.[31] Furthermore, from thermal analysis, it was shown that the crystallization of zirconia occurred at 480 °C in the $ZW_{0.01}$ sample, slightly higher than in the $ZrO_2{\cdot}n(H_2O)$ support (see Table 1). A slight W loading should not influence the temperature of crystallization, because zirconia was detected around 500 °C by Raman spectroscopy during calcination of the $ZW_{0.05}$ sample. Finally, no WO_3 crystallites were detected up to 700 °C, in agreement with XRD data, which only revealed the presence of *t*-ZrO_2 after calcination at 600 and 700 °C (Table 1).

Raman bands are usually downshifted and broadened with an increase in temperature. Indeed, force constants depend on interatomic distances because of anharmonicity of the potential. At the same time, the increase of the breadth of a Raman band is attributed to the decay of a given phonon into two or three phonons.[32] This phenomenon was clearly observed in this study. For instance, the broad-band characteristic of tetragonal zirconia observed near 625 cm^{-1} at 700 °C was blue-shifted and narrowed when the temperature was decreased to 200 °C.

The range above 700 cm^{-1} is free of bands characterizing ZrO_2 and therefore is relevant of the structure of tungsten species. At 147 °C, the splitting of the main band is an indication of a lowering of symmetry that could arise from the bonding of W species with the support. Above 500 °C, the narrow band at 996 cm^{-1} is typical of mono-oxotungsten species. As reported previously,[20] no evidence can be found for the existence of dioxo species, because only one $\nu_{W=O}$ band was clearly evidenced by Raman. Moreover, the slight asymmetry of the band near 1000 cm^{-1} could reveal the presence of various species with different W═O bond orders.[20]

The position of the $\nu_{(W=O)}$ band was shifted from 996 to 1004 cm^{-1} during calcination, and therefore, the bond order increased.[13,20] This band should be shifted to lower frequencies if one only considers the thermal expansion.[32,33] As already observed for the $\nu_{(V=O)}$ band of the monovanadate species,[33] the $\nu_{(W=O)}$ band of calcined W/ZrO_2 samples is downshifted with an increase in temperature. Therefore, the increase in the position of this band during calcination of $ZW_{0.05}$ reveals a structural evolution. This suggests that agglomeration of the tungstate species occurred even if the position of this band remained at a relatively low position. This agglomeration is also evidenced in Table 1. Indeed, the surface area decreased with the rise of the calcination temperature, and consequently, the tungsten surface density increased. However, the strength of the interaction with the support could also influence the position of this band. Indeed, the W═O length of these species depends on the basic strength of the ligands. The larger the basicity is, the lower the W═O frequency that is observed.[34] Finally, the $\nu_{(W=O)}$ shifted at 991 cm^{-1} and was broadened after decreasing the temperature at 200 °C. This phenomenon could be due to the interaction with moisture (see later).

Above 500 °C, the large envelop centered near 840 cm^{-1} contains at least two broad components at 890 and 835 cm^{-1} as the spectra reported by Scheithauer et al.[20] In their paper, the authors proposed that the first band could be due to $\nu_{(W-O-Zr)}$ stretching modes and the other one to $\nu_{(W-O-W)}$ stretching modes. The analogy of the spectra suggests that the samples prepared by anionic exchange or by impregnation contained the same type of species after calcination above 500 °C. On the basis of x-ray absorption near edge structure (XANES) results, Hilbrig et al. proposed five coordinate W species with one W═O bond in the dehydrated state.[35] Iglesia et al. proposed that below typically 4 W/nm^2, the ZrO_2 surface stabilizes dispersed WO_x species which are electronically isolated from each other.[8] Above this value, WO_x species would be more and more agglomerated and some bridging W−O−Zr bonds replaced by some W−O−W linkages. Referring to this typical value, the W surface content of $ZW_{0.05}$ after calcination at 700 °C (see Table 1) indicated that tungsten species were isolated in this sample. However, the presence of the band

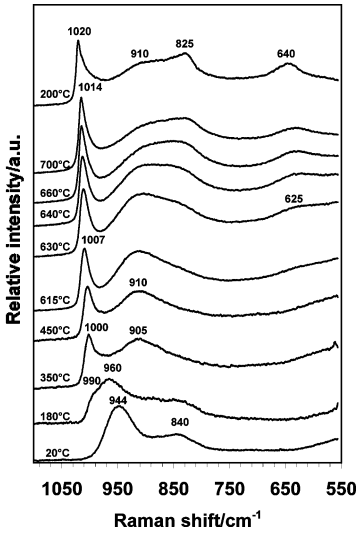

Figure 4. In situ Raman spectra recorded at various temperatures during calcination of $ZrW_{0.25}$ up to 700 °C.

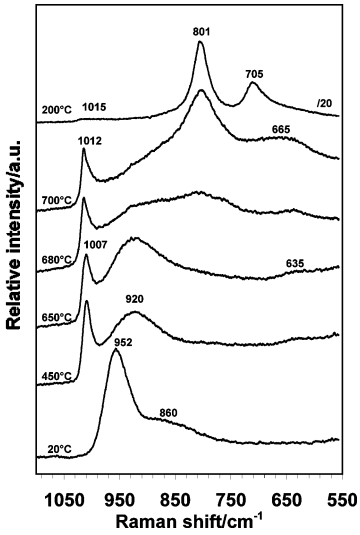

Figure 5. In situ Raman spectra recorded at various temperatures during calcination of ZW_{imp} up to 700 °C.

around 840 cm^{-1} at 508 °C in Figure 3 is in contradiction with the assignment proposed by Scheithauer et al.[20]

Figure 4 shows some spectra recorded during calcination of the $ZW_{0.25}$ sample up to 700 °C. In the same way as the $ZW_{0.05}$ sample, the main band was split at 180 °C. From 200 up to 300 °C, a moderated background of fluorescence was superimposed to Raman bands. Above 300 °C, a narrow band appeared at high frequency. This band shifted from 1000 cm^{-1} at 350 °C to 1014 cm^{-1} at 700 °C. At 350 °C, only one additional band was observed at 905 cm^{-1}. Above 630 °C, two additional bands around 825 and 625 cm^{-1} appeared simultaneously. The last one was due to the crystallization of the *t*-ZrO_2 phase. When the temperature was lowered to 200 °C under ambient air, the bands became more resolved, but the general shape of the spectrum was similar to that recorded at 700 °C. The high-frequency band was then observed at 1020 cm^{-1}.

The evolution of Raman spectra of $ZW_{0.25}$ was different from that of $ZW_{0.05}$. Near 600 °C, the $\nu_{(W=O)}$ stretching band was observed at a slightly higher wavenumber, suggesting a higher degree of agglomeration. This observation is in agreement with the higher value of the W surface content reported in Table 1. Indeed, the significant shift of the high-frequency band fits with the increase of the W surface density from 5.3 up to 7.1 W/nm^2. The presence of tungsten species is known to stabilize the surface area against sintering. This effect is similar to that of sulfates.[4] However, no band typical of *t*-ZrO_2 was observed below 600 °C. As a matter of fact, in a first step, tungsten oxide prevented the nucleation of tetragonal zirconia and the decrease in the surface area. But in a second step, when this nucleation occurred, the higher tungsten surface content favored the agglomeration of WO_x species.

The band near 825 cm^{-1} appeared simultaneously with the bands of *t*-ZrO_2. In the same way, Figure 3 shows that the band near 840 cm^{-1} of $ZW_{0.05}$ was accompanied by the band typical of *t*-ZrO_2 at 508 °C. Scheithauer et al. assigned this band to $\nu_{(W-O-W)}$ stretching modes.[20] According to this proposition, a strong W agglomeration would occur during the nucleation of *t*-ZrO_2. However, such a band was already observed with $ZW_{0.05}$ below 600 °C when the tungsten surface content was low. It can be inferred that this band is due to $\nu_{(W-O-Zr)}$ stretching modes. As a consequence, its position could reveal the strength of the interaction of tungsten species with the support. The band near 900 cm^{-1} would be due to $\nu_{(W-O-W)}$ vibrations. It was clearly observed at 910 cm^{-1} on the $ZW_{0.25}$ sample around 600 °C when the tungsten surface content was already high, in contrast to the $ZW_{0.05}$ sample (see Table 1). In the same way as the $\nu_{(W=O)}$ band, a higher position of the $\nu_{(W-O-W)}$ band should reveal a lower strength of interaction with the support.

The *t*-ZrO_2 phase was also observed by XRD after calcination of $ZW_{0.25}$ at 600 and 700 °C. Its crystallization was not clearly evidenced by thermal analysis.[4] Only a diffuse exothermic phenomenon occurred between 600 and 700 °C followed by an exothermic peak at 710 °C. By Raman spectroscopy, a diffuse band near 625 cm^{-1} was observed at 630 °C. However, its relative intensity remained lower than in the case of $ZW_{0.05}$.

Finally, when the temperature was lowered to 200 °C after calcination in ambient air, the Raman spectrum was different from the corresponding spectrum of $ZW_{0.05}$. At first, the relative intensity of the band around 640 cm^{-1} characteristic of tetragonal zirconia was much lower, possibly because the W surface content was higher after calcination at 700 °C. The high-frequency band remained narrow and shifted upward when the temperature was decreased at 200 °C. This difference of evolution could be explained by the presence of different types of species.

The evolution of the Raman spectra of ZW_{imp} during calcination is reported in Figure 5. From 200 up to 320 °C, a very strong fluorescence was observed, and the Raman bands were revealed with difficulty. Above 320 °C, a narrow band at 1007 cm^{-1} and a broad band around 920 cm^{-1} were observable. At 450 °C, a very small band was distinguishable near 635 cm^{-1}. From 450 up to 650 °C, the evolution was similar to that observed with $ZW_{0.25}$. However, the two bands were shifted to higher wavenumbers. Above 680 °C, the evolution was completely different. In particular, the narrow band shifted to 1013 cm^{-1}, and two broad and intense bands appeared around 800 and 655 cm^{-1}. When the temperature was lowered to 200 °C under ambient air, their relative intensities became much higher and they were located at 801 and 705 cm^{-1}. In addition, the yellow color of this sample after calcination indicated the presence of WO_3 crystallites.

The Raman bands which appeared at 680 °C could correspond to the α tetragonal structure of WO_3.[36,37] This structure is stable above 900 °C when the crystallite size is typically 500 nm.[36] However, when this size is lower, the tetragonal phase is stable at lower temperatures. For instance, when the crystallite size is

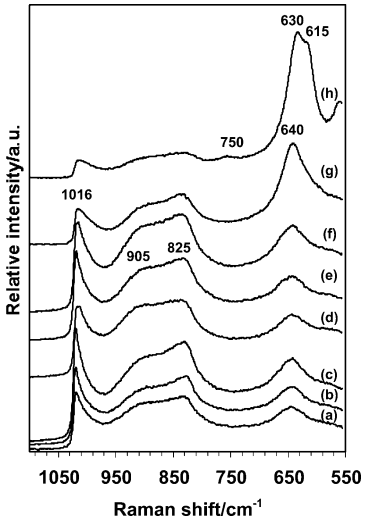

Figure 6. Raman spectra recorded on various points ((a) to (h)) of $ZW_{0.25}$ powder at 200 °C after calcination at 700 °C.

60 nm, it is observed above 680 °C. When the temperature is lowered to 200 °C, a phase transition to the β orthorhombic structure and then another to the γ monoclinic structure occur.[36] In these structures, slightly distorted WO_6 octahedra are linked by the corners, and there is no W═O bond. That is the reason no stretching vibrations are observed above 820 cm^{-1}. The two bands located at 801 and 705 cm^{-1} observed at 200 °C after calcination of ZW_{imp} are typical of this γ monoclinic structure.

The observation by Raman spectroscopy of the nucleation of WO_3 at 680 °C is in agreement with the results reported in ref 20. Accordingly, the XRD pattern recorded on the ZW_{imp} sample after calcination at 800 °C evidenced the presence of γ-WO_3, indicating that the nucleation of this phase occurred at a lower temperature. By thermal analysis of ZW_{imp}, two exothermic peaks were evidenced at 440 and 710 °C. They could arise from the crystallization of ZrO_2 and WO_3, respectively.[4] The Raman spectra recorded during the calcination of this sample are in agreement with this analysis, because a weak band near 640 cm^{-1} characterizing zirconia was observed at 450 °C and the crystallization of WO_3 was evidenced at 680 °C. In the same way as $ZW_{0.25}$, the weak relative intensity of the band typical of *t*-ZrO_2 could reveal a high tungsten surface density.

As already proposed, the positions of the $\nu_{(W=O)}$ and $\nu_{(W-O-W)}$ bands could indirectly reveal the strength of the interaction with the support. The ZW_{imp} and $ZW_{0.25}$ samples contained the same W amount. At 450 °C, the $\nu_{(W=O)}$ and $\nu_{(W-O-W)}$ bands of ZW_{imp} were observed at 1007 and 920 cm^{-1} versus 1000 and 905 cm^{-1} in the case of $ZW_{0.25}$. It suggests that the interaction with the support was weaker in the impregnated sample. Interestingly, WO_3 was nucleated at a lower temperature. At 700 °C, the $\nu_{(W=O)}$ band was located at lower frequency than the corresponding band of $ZW_{0.25}$, probably because the surface density of supported W species was lower after the crystallization of WO_3.

Figure 6 shows the high homogeneity of the samples prepared by anionic exchange. The figure presents eight spectra recorded at 200 °C on $ZW_{0.25}$ under ambient air by moving the position of the laser spot on the powder bed and optimizing the focus each time. The spectra a to g evidenced four bands around 1014, 905, 825, and 640 cm^{-1}. However, some slight differences can be distinguished. For instance, the relative intensity of the band at 905 cm^{-1} is higher in spectrum d, and two $\nu_{(W=O)}$ bands were located at 1016 and 1012 cm^{-1}. Spectrum g is also slightly different, because the band at 640 cm^{-1} is better defined and its relative intensity higher. This can be explained by better crystallinity of ZrO_2. Spectrum h was recorded on a particular point. Indeed, two bands and also an overtone typical of the monoclinic ZrO_2 structure were observed at 630 and 615 cm^{-1} [28,30] and at 750 cm^{-1}, respectively.[20]

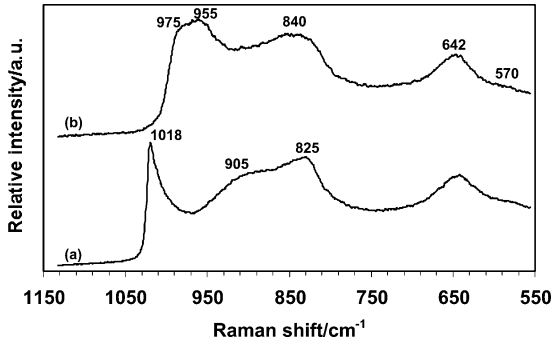

Figure 7. Raman spectra of $ZW_{0.25}$ at (a) 200 °C and (b) room temperature.

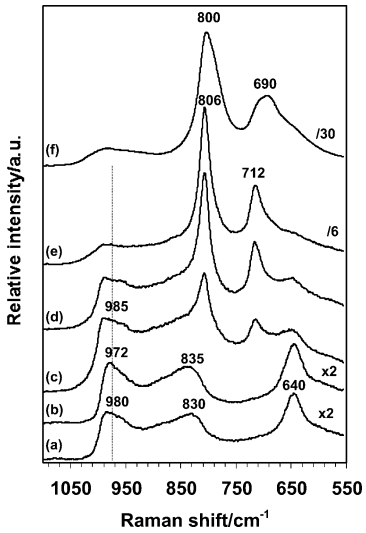

Figure 8. Raman spectra recorded on various points ((a) to (f)) of ZW_{imp} at room temperature after calcination at 700 °C.

The influence of hydration on Raman spectra of W/ZrO_2 compounds is underlined in Figure 7. The spectra of $ZW_{0.25}$ recorded at 200 °C and at room temperature in air after calcination both contained a band near 640 cm^{-1}. However, above 800 cm^{-1}, the shape of the spectrum is completely different. The narrow band at 1018 cm^{-1} disappeared through rehydration and was replaced by two badly defined bands at 975 and 955 cm^{-1}. This observation confirmed that W species were located on the support and were accessible for interaction with water molecules.[20,38] This phenomenon has been reported to be due to the formation of $W^{6+}-OH$ from water-dissociative adsorption.[13,39] The positions of these bands are shifted upward with the surface tungsten content and the degree of condensation.[16,20,40] The observation of two bands could be attributed to two hydrated mono-oxo species with various bond orders.[20] Interestingly, similar bands were observed on WO_3 hydrates in both the IR and Raman spectra[13] and on WO_3 nanocrystallites of 4 nm.[36]

Several points of $ZW_{0.25}$ were analyzed by micro-Raman after calcination at room temperature under ambient air and revealed also a good homogeneity. On the contrary, six spectra were recorded on the ZW_{imp} powder after calcination at 700 °C and rehydration. They are presented in Figure 8. Two kinds of spectra were obtained: the first presents three bands at 640,

835, and 970−980 cm^{-1} (spectra a and b). They are typical of polymeric W species supported on *t*-ZrO_2. The other kind is mainly dominated by two very intense bands around 800 and 712 cm^{-1} of γ-WO_3 (spectrum e). Spectra c and d correspond to a mixture of these typical spectra. The position of the high-frequency band varied from 972 to 985 cm^{-1}, revealing various degrees of condensation of the supported species and thus a structural heterogeneity. Finally, spectrum f, which shows broad bands around 800 and 685 cm^{-1}, was recorded on a particular point. It could be due to the presence of $WO_3 \cdot {}^1/_3H_2O$ particles.[41,42]

Conclusion

The structural evolution of WO_x/ZrO_2 catalysts prepared by anionic exchange was studied by in situ Raman spectroscopy. This novel method of preparation corresponds to an anionic exchange of peroxotungstate species with hydroxyl groups of zirconium hydroxide. A reference sample was also prepared by impregnation and characterized for comparison.

$(W_2O_3(O_2)_4(H_2O)_2)^{2-}$ was the main species identified in all the $H_2WO_4-H_2O_2$ precursor solutions, even for low H_2O_2/W ratios. This low-nuclearity species was then exchanged with $ZrO_2 \cdot n(H_2O)$, and the resulting tungstate compounds were dried.

The Raman spectra of the exchanged samples evidenced bands typical of the internal vibrations of WO_4^{2-} tetrahedra. At high W loading, the main band was slightly shifted to higher frequency, revealing an aggregation of tungsten species. However, this aggregation was limited with regard to the impregnated species. Therefore, the method of preparation determines the nature of the W species in the dried compounds. According to the nature of these species, the catalytic properties for dibenzothiophene oxidation are totally different.

The differences between the exchanged and the impregnated catalysts are less pronounced after calcination. All the samples evidenced tungsten species with one W═O bond in the dehydrated state. The Raman monitoring of $ZW_{0.05}$ during calcination up to 700 °C evidenced the formation of tetragonal zirconia. The band appearing at 840 cm^{-1} simultaneously with the bands characteristic of the tetragonal zirconia is tentatively assigned to $\nu_{(W-O-Zr)}$ vibrations. On the contrary, the spectra of $ZW_{0.25}$ evidenced, at temperatures lower than 615 °C, only the $\nu_{(W=O)}$ band and a broad band near 910 cm^{-1} that could be attributed to W−O−W bonds. Above 615 °C, the *t*-ZrO_2 phase crystallized, and simultaneously, a band at 825 cm^{-1} appeared. The higher position of the $\nu_{(W=O)}$ band is an indication of a lower W dispersion. The spectral evolution of ZW_{imp} during calcination was, at low temperature, very similar to that of $ZW_{0.25}$. However, the positions of the $\nu_{(W=O)}$ and $\nu_{(W-O-W)}$ vibrations were higher at 450 °C, suggesting that the interaction with the support was weaker in the impregnated sample, and interestingly, the formation of WO_3 was evidenced at only 680 °C. The spectra recorded at room temperature under ambient air confirmed the role of water on the structure of W-supported species. The spatial Raman characterization obtained on various points indicated the enhanced homogeneity of the exchanged catalysts compared to the impregnated one.

References and Notes

(1) Hino, M.; Arata, K. *J. Chem. Soc., Chem. Commun*. **1987**, 1259.

(2) Arata, K.; Hino, M. In *Proceedings of the 9th International Congress on Catalysis*, Calgary, 1988; Phillips, M. J., Ternan, M., Eds.; The Chemical Institute of Canada: Ottawa, 1988; p 1727.

(3) Figueras, F.; Essayem, N.; Feche, C.; Loridant, S.; Palomeque, J.; Gelbard, G. Fr. Patent 02 08318, 2002.

(4) Figueras, F.; Palomèque, J.; Loridant, S.; Fèche, C.; Essayem, N.; Gelbard G. *J. Catal.* **2004**, *226*, 25.

(5) Fèche, C. Ph.D. Thesis, Université Lyon 1, 2004.

(6) Banares, M. A.; Wachs I. E. *J. Raman Spectrosc.* **2002**, *33*, 359.

(7) Wachs, I. E.; Weckhuysen B. M. *Appl. Catal., A* **1997**, *157*, 67.

(8) Barton, D. G.; Shtein, M.; Wilson, R. D.; Soled, S. L.; Iglesia, E. *J. Phys. Chem. B* **1999**, *103*, 630.

(9) Barton, D. G.; Soled, S. L.; Meitzer, G. D.; Fuentes, G. A.; Iglesia, E. *J. Catal.* **1999**, *181*, 57.

(10) Barton, D. G.; Soled, S. L.; Iglesia, E. *Topics Catal.* **1998**, *6*, 87.

(11) Tichit, D.; El Alami, D.; Figueras, F. *Appl. Catal., A* **1996**, *145*, 195.

(12) Campbell, N. J.; Dengel, A. C.; Edwards, C. J.; Griffith, W. P. *J. Chem. Soc., Dalton Trans.* **1989**, *6*, 1203.

(13) Busca, G. *J. Raman Spectrosc.* **2002**, *33*, 348.

(14) Contant, R.; Thouvenot, R. *Inorg. Chim. Acta* **1993**, *212*, 41.

(15) Aubry, C.; Chottard, G.; Platzer, N.; Brégeault, J.-M.; Thouvenot, R.; Chauveau, F.; Huet, C.; Ledon, H. *Inorg. Chem*. **1991**, *30*, 4409.

(16) Gazzoli, D.; Valigi, M.; Dragone, R.; Marucci, A.; Mattei, G. *J. Phys. Chem. B* **1997**, *101*, 11129.

(17) Ng, K. Y. S.; Gulari, E. *Polyhedron* **1984**, *3(8)*, 1001.

(18) Griffith, W. P.; Lesniak, P. J. B. *J. Chem. Soc., A* **1969**, 1066.

(19) Nyquist, R. A.; Putzig C. L.; Leugers, M. A. *Handbook of Infrared and Raman spectra of inorganic compounds and organic salts*; Academic Press: New York, 1997; p 18.

(20) Scheithauer, M.; Grasselli, R. K.; Knözinger, H. *Langmuir* **1998**, *14*, 3019.

(21) Okada, K.; Morikawa, H.; Marumo, F.; Iwai S. *Acta Crystallogr., Sect. B* **1974**, *30*, 1872.

(22) Guermen, E.; Daniels, E.; King J. S. *J. Chem. Phys.* **1971**, *55(3)*, 1093.

(23) Christofilos, D.; Papagelis, K.; Ves, S.; Kourouklis, G. A.; Raptis, C. *J. Phys.: Condens. Matter* **2002**, *14*, 12641.

(24) Schofield, P. F.; Knight, K. S.; Redfern, S. A. T.; Cressey, G. *Acta Crystallogr., Sect. B* **1997**, *53(1)*, 102.

(25) Liegeois-Duyckaerts, M.; Tarte, P. *Spectrochim. Acta, Part A* **1972**, *28*, 2029.

(26) Ravindran, T. R.; Arora, A. K.; Mary, T. A. *J. Phys.: Condens. Matter* **2001**, *13*, 11573.

(27) Hanuza, J.; Maczka, M.; Hermanowicz, K.; Andruszkiewicz, M.; Pietraszko, A.; Strek, W.; Deren, P. *J. Solid State Chem.* **1993**, *105*, 49.

(28) Djurado, E.; Bouvier, P.; Lucazeau, G. *J. Solid State Chem*. **2000**, *149*, 399.

(29) Bouvier, P.; Godlewski, J.; Lucazeau, G. *J. Nucl. Mater.* **2002**, *300*, 118.

(30) Zhao, B.; Xu, X.; Gao, J.; Fu, Q.; Tang, Y. *J. Raman Spectrosc.* **1996**, *27*, 549.

(31) Kuba, S.; Concepcion Heydorn, P.; Grasselli, R. K.; Gates, B. C.; Che, M.; Knözinger, H. *Phys. Chem. Chem. Phys.* **2001**, *3*, 146.

(32) Lucazeau, G. *J. Raman Spectrosc.* **2003**, *34(7/8)*, 478.

(33) Xie, S.; Iglesia, E.; Bell, A. T. *J. Phys. Chem. B* **2001**, *105*, 5144

(34) Gutiérrez-Alejandre, A.; Castillo, P.; Ramirez, J.; Ramis, G.; Busca, G. *Appl. Catal., A* **2001**, *216*, 181.

(35) Hilbrig, F.; Göbel, H. E.; Knözinger, H.; Schmelz, H.; Lengeler, B. *J. Phys. Chem.* **1991**, *95*, 6973.

(36) Boulova, M.; Lucazeau, G. *J. Solid State Chem.* **2002**, *167*, 425.

(37) Gabrusenoks, J.; Veispals, A.; von Czarnowski, A.; Meiwes-Broer, K.-H. *Electrochim. Acta* **2001**, *46*, 2231.

(38) Scheithauer, M.; Grasselli, R. K.; Knözinger, H. *Prepr.—Amer. Chem. Soc.* **1997**, *42(4)*, 738.

(39) Boulova, M.; Gaskov, A.; Lucazeau, G. *Sens. Actuators, B* **2001**, *81*, 99.

(40) Vaidyanathan, N.; Hercules, D. M.; Houalla, M. *Anal. Bioanal. Chem.* **2002**,

(41) Daniel, M. F.; Desbat, B.; Lassegues, J. C.; Gerand, B.; Figlarz, M. *J. Solid State Chem.* **1987**, *67*, 235.

(42) Delichere, P.; Falaras, P.; Froment, M.; Le Goff, A. H. *Thin Solid Films* **1988**, *161*, 35.